

RESEARCH

Open Access



Associations of MRI-visible perivascular spaces with longitudinal cognitive decline across the Alzheimer's disease spectrum

Ming-Liang Wang¹, Qiao-Qiao Zou¹, Zheng Sun¹, Xiao-Er Wei¹, Peng-Yang Li², Xue Wu³, Yue-Hua Li^{1*} and for the Alzheimer's Disease Neuroimaging Initiative

Abstract

Objective: To investigate the characteristics and associations of MRI-visible perivascular spaces (PVS) with clinical progression and longitudinal cognitive decline across the Alzheimer's disease spectrum.

Methods: We included 1429 participants (641 [44.86%] female) from the Alzheimer's Disease Neuroimaging Initiative (ADNI) database. PVS number and grade in the centrum semiovale (CSO-PVS), basal ganglia (BG-PVS), and hippocampus (HP-PVS) were compared among the control (CN), mild cognitive impairment (MCI), and Alzheimer's disease (AD) groups. PVS were tested as predictors of diagnostic progression (i.e., CN to MCI/AD or MCI to AD) and longitudinal changes in the 13-item Alzheimer's Disease Assessment Scale-cognitive subscale (ADAS-Cog 13), Mini-Mental State Examination (MMSE), memory (ADNI-MEM), and executive function (ADNI-EF) using multiple linear regression, linear mixed-effects, and Cox proportional hazards modeling.

Results: Compared with CN subjects, MCI and AD subjects had more CSO-PVS, both in number ($p < 0.001$) and grade ($p < 0.001$). However, there was no significant difference in BG-PVS and HP-PVS across the AD spectrum ($p > 0.05$). Individuals with moderate and frequent/severe CSO-PVS had a higher diagnostic conversion risk than individuals with no/mild CSO-PVS (log-rank $p < 0.001$ for all) in the combined CN and MCI group. Further Cox regression analyses revealed that moderate and frequent/severe CSO-PVS were associated with a higher risk of diagnostic conversion (HR = 2.007, 95% CI = 1.382–2.914, $p < 0.001$; HR = 2.676, 95% CI = 1.830–3.911, $p < 0.001$, respectively). A higher CSO-PVS number was associated with baseline cognitive performance and longitudinal cognitive decline in all cognitive tests ($p < 0.05$ for all).

Conclusions: CSO-PVS were more common in MCI and AD and were associated with cognitive decline across the AD spectrum.

Keywords: Perivascular spaces, MRI, Alzheimer's disease, Cognitive impairment, Conversion

Introduction

Alzheimer's disease (AD) is the most common cause of dementia and is becoming one of the most expensive and lethal diseases, resulting in a great social burden [1]. The pathophysiology of AD is mainly characterized by amyloid- β (A β) plaques, hyperphosphorylated tau, and neuroinflammation [1]. However, pharmacotherapies targeting A β and tau have achieved limited success [2].

*Correspondence: liyuehua312@163.com

¹ Department of Radiology, Shanghai Sixth People's Hospital Affiliated to Shanghai Jiao Tong University School of Medicine, No. 600, Yi Shan Road, Shanghai 200233, China
Full list of author information is available at the end of the article



© The Author(s) 2022. **Open Access** This article is licensed under a Creative Commons Attribution 4.0 International License, which permits use, sharing, adaptation, distribution and reproduction in any medium or format, as long as you give appropriate credit to the original author(s) and the source, provide a link to the Creative Commons licence, and indicate if changes were made. The images or other third party material in this article are included in the article's Creative Commons licence, unless indicated otherwise in a credit line to the material. If material is not included in the article's Creative Commons licence and your intended use is not permitted by statutory regulation or exceeds the permitted use, you will need to obtain permission directly from the copyright holder. To view a copy of this licence, visit <http://creativecommons.org/licenses/by/4.0/>. The Creative Commons Public Domain Dedication waiver (<http://creativecommons.org/publicdomain/zero/1.0/>) applies to the data made available in this article, unless otherwise stated in a credit line to the data.

Other upstream mechanisms, such as glymphatic dysfunction [3] and other clearance system damage, might also affect the clinical development of AD.

MRI-visible perivascular spaces (PVS) are fluid-filled spaces surrounding small penetrating blood vessels, which can be observed on brain MRI [4, 5]. Traditionally, MRI-visible PVS was regarded as an imaging marker of small vessel disease and correlated with aging [6]. However, the perivascular space has been increasingly suggested to play an important part in the glymphatic system, through which brain waste products are cleared from the brain [7, 8]. Impairment of the glymphatic system may lead to perivascular space enlargement and reduce the clearance of brain waste products, which would further lead to retrograde enlargement of the perivascular space [9]. Several studies have found associations between MRI-visible PVS and neurodegenerative diseases, including Parkinson's disease [10–12], Huntington's disease [13], frontotemporal lobar degeneration [14], and Fabry disease [15]. A previous study even found an association between MRI-visible PVS and brain tau deposition in a normal older population [16] and in military veterans with traumatic brain injury [17].

There have been cross-sectional studies with small samples (less than 200 subjects) investigating the relationship between MRI-visible PVS and AD [18–21]. However, the results of these studies were mixed, as some studies found more MRI-visible PVS in AD patients than in normal controls, while some studies did not. Furthermore, no specific study has investigated the role of MRI-visible PVS in predicting clinical progression and longitudinal cognitive change across the AD spectrum. In this longitudinal study, we aimed to investigate the distribution characteristics of MRI-visible PVS and the associations with cognitive decline and clinical progression across the AD spectrum.

Materials and methods

Study subjects

Data used in this study were obtained from the Alzheimer's Disease Neuroimaging Initiative (ADNI) database, led by Principal Investigator Michael W. Weiner, M (<http://adni.loni.usc.edu>). The ADNI project was launched in 2003 and was designed to measure the progression of mild cognitive impairment and early Alzheimer's disease by investigating serial MRI, PET, biological markers, and clinical and neuropsychological assessments. The ADNI study was approved by the institutional review boards of all participating institutions. Written informed consent was obtained from all the participants or their authorized representatives in accordance with the Declaration of Helsinki.

The specific enrolment procedure and inclusion criteria for the different diagnostic categories in the ADNI cohort have been described previously [22]. All subjects were classified as control (CN), mild cognitive impairment (MCI), or AD at each visit. CN subjects had normal cognitive function, with a Mini-Mental State Examination (MMSE) score of 24–30 and a clinical dementia rating (CDR) score of 0. MCI subjects had an MMSE score of 24–30, a global CDR of 0.5, and a memory box score of at least 0.5. AD subjects had an MMSE score of 20–26 and a global CDR \geq 0.5. Subjects diagnosed with EMCI or LMCI on the ADNI-2 were also considered to have MCI.

All study subjects who had a baseline brain MRI examination including T1-weighted, T2-weighted, and T2 fluid-attenuated inversion recovery (FLAIR) sequences were included from the ADNI database. The data from the ADNI-1 and ADNI-2 fulfilled these inclusion criteria and were used in this study. The time interval between MRI examination and baseline cognitive tests was within 1 month. We excluded 77 subjects with low MR image quality, and there was no significant difference between the included and excluded subjects in the CN, MCI, and AD groups (Supplementary Table 1). Finally, a total of 1429 individuals (486 CN, 667 MCI, and 276 AD) were included in this study.

Clinical and cognitive assessments

We used multiple scales to assess cognitive functions, including global cognition by the 13-item AD Assessment Scale-cognitive subscale (ADAS-Cog 13) and MMSE. The ADNI memory composite score (ADNI-MEM), based on the Rey Auditory Verbal Learning task, word list learning and recognition tasks from ADAS-Cog, recall from Logical Memory I of the Wechsler Memory Test–Revised, and the 3-word recall item from the MMSE, was used to assess memory [23]. Executive function was assessed by the ADNI executive function score (ADNI-EF), which consisted of Category Fluency, Digit Span Backwards, Trail-Making Test Parts A and B, Wechsler Adult Intelligence Scale–Revised Digit–Symbol Substitution, and Clock Drawing items [24]. The baseline and the longest follow-up cognitive test data were collected.

Participant status at each visit was recorded as stable, reverted, or converted, with the former two statuses considered no progression and the latter considered progression, including CN conversion to MCI/AD and MCI conversion to AD. The last visit was used to determine the final diagnosis status for survival analysis. Notably, the definition of clinical progression was strictly defined beforehand in our study. For subjects who first progressed to MCI/AD and then reverted to their previous status, the first conversion to MCI/AD was not considered an event, as there may have been a mistake in the

evaluation of the participant status. The progression time was calculated as the interval between the participant's visit date when the conversion occurred and the baseline visit data.

MRI acquisition and analysis

MR examinations were performed according to the ADNI MRI scanning protocol. Two trained neuroradiologists (M.L.W. and X.E.W. with 10 and 15 years of experience, respectively) who were blinded to the clinical diagnosis, demographic characteristics, and cognitive test results assessed the MR images according to the Standards for Reporting Vascular Changes on Neuroimaging (STRIVE) [25].

The T1-weighted, T2-weighted, and T2 FLAIR sequences of the baseline MR images were comprehensively assessed for the existence of PVS, and the T2-weighted sequence was specifically used for counting PVS. MRI-visible PVS were located along the penetrating arteries and were characterized as round, ovoid, or linear lesions with a high signal on T2-weighted images and low signals on T1-weighted and FLAIR images (Fig. 1). PVS number was evaluated in the centrum semiovale (CSO), basal ganglia (BG), and hippocampus (HP). Furthermore, a validated 5-point visual rating scale was used to evaluate PVS severity (0 = no PVS, 1 = 1–10 PVS, 2 = 11–20 PVS, 3 = 21–40 PVS, and 4 = more than 40 PVS) for CSO-PVS and BG-PVS [26, 27]. Categories 0 and 1 were collapsed to no/mild severity; category 2 was classified as moderate severity; and categories 3 and 4 were classified as frequent/severe level. HP-PVS were subdivided by the number of PVS into no/mild severity (0–1 PVS), moderate severity (2–4 PVS), and frequent/severe level (>4 PVS) [21] (Fig. 1). White matter hyperintensity (WMH) volume and total intracranial volume were obtained; the method is described on the ADNI website (<http://adni.loni.usc.edu>, “4-Tissue Segmentation Methods for ADNI MR Scans.pdf”). The WMH volumes were nonnormally distributed and thus were log-transformed for analysis. The hippocampus volume was also extracted using the FreeSurfer method (<http://adni.loni.usc.edu>, “UCSF FreeSurfer Methods.pdf”).

The interrater reliability was excellent for the CSO-PVS number [intraclass correlation coefficient (ICC) = 0.936, 95% CI: 0.929–0.942], BG-PVS number (ICC = 0.903, 95% CI: 0.893–0.912), and HP-PVS number (ICC = 0.912, 95% CI: 0.903–0.921). The intra-rater reliability was determined from a random sample of 100 subjects with a 1-month interval between the first and second image assessments performed by the senior neuroradiologist. The intra-rater reliability was also excellent for the CSO-PVS number (ICC = 0.942, 95% CI: 0.915–0.961), BG-PVS number (ICC = 0.928, 95% CI: 0.895–0.951),

and HP-PVS number (ICC = 0.920, 95% CI: 0.884–0.946). The PVS rating scale of the senior radiologist was used for the analysis.

Statistical analysis

All statistical tests were performed by IBM SPSS Statistics for Windows, version 20.0, and R software (version 3.3.0; Vienna, Austria). Categorical variables were expressed as numbers (percentages) and were compared using the chi-square test among the CN, MCI, and AD groups. WMH and follow-up months were nonnormally distributed and thus were expressed as median [interquartile range (IQR)]. WMH volume was also log-transformed for further analysis. Other quantitative variables, including age, education, cognitive test scores, PVS number, HP volume, and intracranial volume, were expressed as the mean (standard deviation). Analyses of variance (ANOVAs) were used in the comparisons of all quantitative variables among the CN, MCI, and AD groups. Post hoc multiple comparisons were performed with Bonferroni tests.

The Kaplan–Meier method plotted with log-rank tests was used to investigate the association between MRI-visible PVS and clinical progression in the combined CN and MCI group. A Cox proportional hazard regression model was further conducted to estimate the hazard ratio (HR) with a 95% confidence intervals (CIs), adjusted by age, sex, education, APOε4, hypertension, diabetes, hyperlipidemia, coronary heart disease, atrial fibrillation, smoking, WMH volume, hippocampus volume, and intracranial volume. The three-level ordinal form of MRI-visible PVS was used. The no/mild severity group was set as the reference group, and the other groups were dummy coded for the survival analyses. The Cox proportional hazards assumption was assessed with the Schoenfeld residuals test, and all of the factors satisfied the proportional hazards hypothesis ($p > 0.05$ for all). Individuals who did not develop MCI/AD were censored at the time of their last evaluation. These analyses were also performed for the CN and MCI groups separately.

Multivariable linear regression analyses were used to estimate the association between MRI-visible PVS number and baseline cognitive test performance. Linearity, normality, independence, and variance homogeneity were all fulfilled for the multivariable linear regression. To examine clinical progression in detail, we performed linear mixed-effects (LME) models with ADAS-Cog 13, MMSE, ADNI-MEM, and ADNI-EF as outcome variables and PVS number, time, and PVS number \times time as predictors. The interaction term PVS number \times time was the effect of interest, as it reflected whether MRI-visible PVS number moderated the relationship between time and cognitive performance. Our models contained

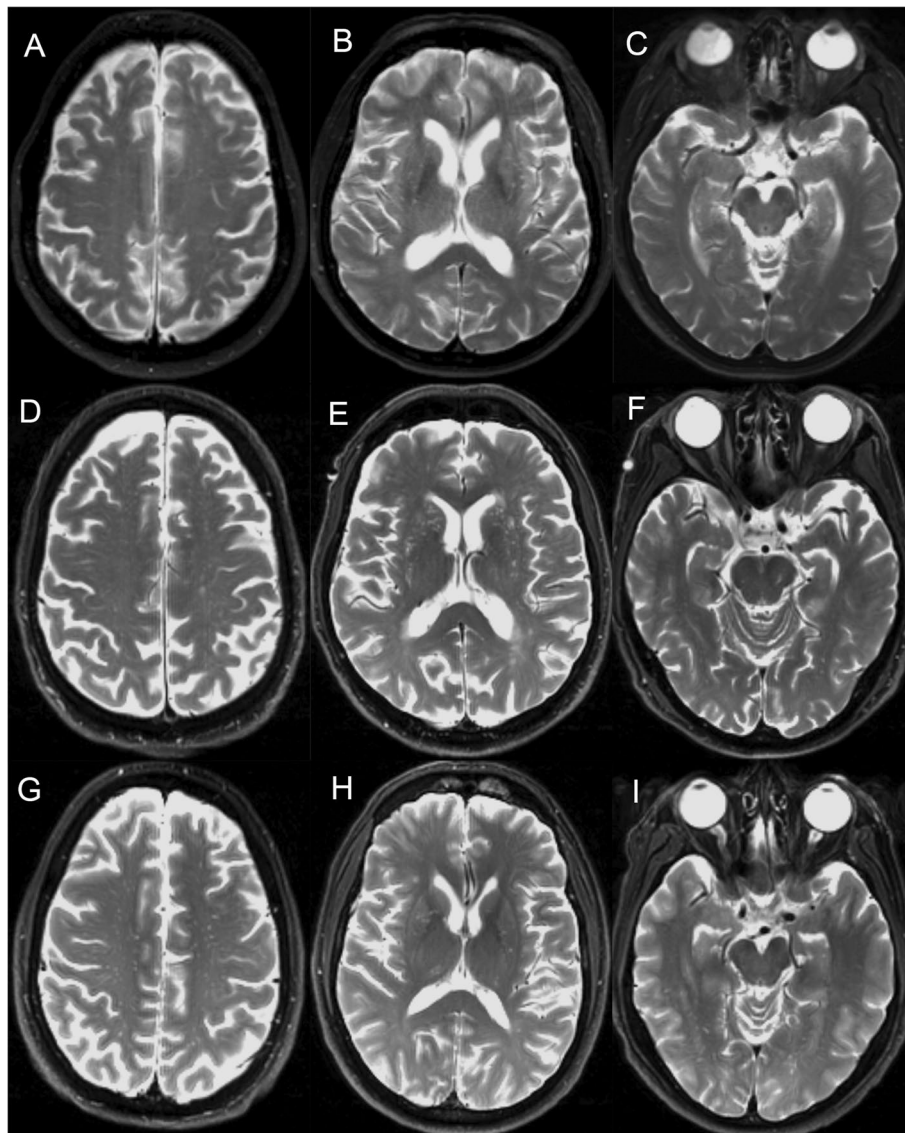


Fig. 1 Examples of MRI-visible PVS across the AD spectrum. **A–C** A female control subject aged 78 had mild grade CSO-PVS, mild grade BG-PVS, and frequent/severe grade HP-PVS. After a follow-up of 24 months, this subject did not convert into MCI or AD. **D–F** A male MCI subject aged 75 had frequent/severe grade CSO-PVS, frequent/severe grade BG-PVS, and none HP-PVS. After a follow-up of 54 months, this subject converted into AD. **G–I** A male AD subject aged 62 had frequent/severe grade CSO-PVS, moderate grade BG-PVS, and mild grade HP-PVS. CN control, MCI mild cognitive impairment, AD Alzheimer disease, CSO centrum semiovale, BG basal ganglia, HP hippocampus, PVS perivascular spaces

random intercepts and slopes. Normality was fulfilled for the LME models. All the regression models included the following covariates: age, sex, education, APO ϵ 4, hypertension, diabetes, hyperlipidemia, coronary heart disease, atrial fibrillation, smoking, WMH volume, hippocampus volume, and intracranial volume, as these covariates may affect cognitive changes. Continuous independent variables and covariates in the models were z-scored prior to analysis for standardization. The regression model results are shown as beta coefficients, 95% CIs, and p values,

and a forest plot was created for the whole-group LME model. $p < 0.05$ derived from two-tailed tests was considered statistically significant.

Results

Participant characteristics

Participant demographics and cognitive performance are shown in Table 1. Compared with CN subjects, MCI subjects were younger ($p = 0.017$). There were fewer female subjects in the MCI group than in the CN group

Table 1 Demographics and clinical characteristics across the Alzheimer's disease spectrum

Characteristics	Data available	CN	Data available	MCI	Data available	AD	<i>p</i> value
Age (years)	486	75.0 (5.8)	667	74.0 (7.4)	276	75.1 (7.8)	0.017 ^{*a}
Sex, female <i>n</i> (%)	486	251 (51.6)	667	263 (39.4)	276	127 (46.0)	<0.001 ^{*a}
Education (years)	486	16.3 (2.7)	667	16.0 (2.9)	276	15.1 (3.0)	<0.001 ^{*a,b,c}
APOE ε4 carriers <i>n</i> (%)	486	140 (28.8)	667	348 (52.2)	276	186 (67.4)	<0.001 ^{*a,b,c}
Hypertension, <i>n</i> (%)	486	238 (49.0)	667	331 (49.6)	276	138 (50.0)	0.958
Diabetes mellitus, <i>n</i> (%)	486	39 (8.0)	667	56 (8.4)	276	19 (6.9)	0.737
Hyperlipidemia, <i>n</i> (%)	486	215 (44.2)	667	306 (45.9)	276	134 (48.6)	0.517
Coronary heart disease, <i>n</i> (%)	486	30 (6.2)	667	44 (6.6)	276	14 (5.1)	0.675
Atrial fibrillation, <i>n</i> (%)	486	21 (4.3)	667	25 (3.7)	276	9 (3.3)	0.752
Smoking, <i>n</i> (%)	486	194 (39.9)	667	265 (39.7)	276	100 (36.2)	0.549
Cognition							
Baseline ADAS-Cog 13	484	9.21 (4.31)	657	17.26 (6.69)	261	29.53 (7.91)	<0.001 ^{*a,b,c}
Baseline MMSE score	486	29.0 (1.18)	666	27.1 (2.14)	276	22.9 (2.99)	<0.001 ^{*a,b,c}
Baseline ADNI-MEM score	483	1.07 (0.59)	656	0.069 (0.77)	265	-0.87 (0.57)	<0.001 ^{*a,b,c}
Baseline ADNI-EF score	483	0.77 (0.83)	656	0.12 (0.96)	265	-0.96 (0.94)	<0.001 ^{*a,b,c}
Clinical progression							
Follow-up, months		36 (24, 60)		27 (18, 36)			<0.001 [*]
Conversion to MCI, <i>n</i> (%)		77 (16.3)					
Conversion to AD, <i>n</i> (%)		10 (2.1)		273 (42.5)			

Values are reported as mean (standard deviation) for the quantitative variables except follow-up month which is reported as median (interquartile range). Categorical variables are reported as frequency (percentage). ^{*}*p* < 0.05. Group comparisons were done with the one-way ANOVA (quantitative variables) and chi-square test (categorical variables). ^a*p* < 0.05 between CN vs MCI. ^b*p* < 0.05 between CN vs AD. ^c*p* < 0.05 between MCI vs AD. CN control, MCI mild cognitive impairment, AD Alzheimer disease, ADAS-Cog 13 13-item Alzheimer's Disease Assessment Scale-cognitive subscale, MMSE Mini-Mental State Examination, ADNI-MEM ADNI memory composite score, ADNI-EF ADNI executive function score, ADNI Alzheimer's Disease Neuroimaging Initiative

(*p* < 0.001). The MCI and AD groups were less educated and had more APOE ε4 carriers than the CN group (*p* < 0.001 for all). There was no significant difference in smoking status or cardiovascular disease history (*p* > 0.05 for all). On all cognitive measures, there were significant baseline differences between disease stages (*p* < 0.001 for all). After 36 (median) (IQR, 24–60) months of follow-up, 77 CN subjects (16.3%) converted to MCI status, and 10 CN subjects (2.1%) converted to AD status. In the MCI group, 273 subjects (42.5%) converted to AD status after a follow-up of 27 (median) (IQR, 18–36) months.

Group comparisons and distribution characteristics of MRI-visible PVS across the AD spectrum

Table 2 shows the group comparisons and distribution characteristics of MRI-visible PVS and other neuroimaging findings across the AD spectrum. Compared with CN subjects, MCI and AD subjects had more CSO-PVS, both in number (*p* < 0.001) and grade (*p* < 0.001). However, there was no significant difference in BG-PVS and HP-PVS across the AD spectrum (*p* > 0.05 for all). Furthermore, MCI and AD subjects had smaller hippocampal volumes than CN subjects (*p* < 0.001). Compared with CN subjects, MCI subjects had a larger intracranial

volume (*p* = 0.005). There was no significant difference in WMH volume (*p* > 0.05).

MRI-visible PVS and risks of diagnostic conversion into MCI/AD

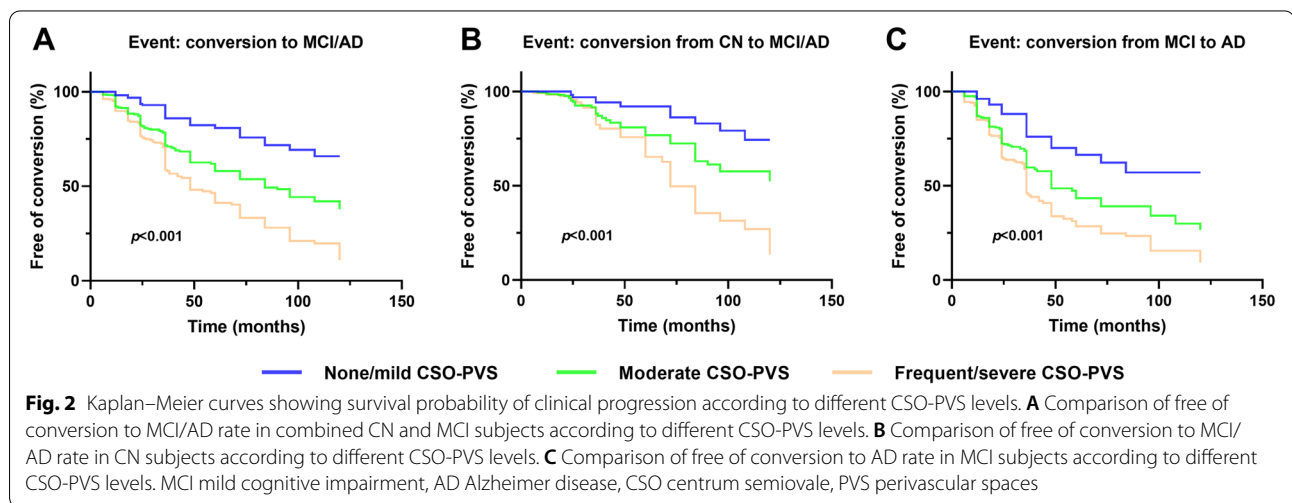
The Kaplan–Meier curves of diagnostic conversion according to the grades of CSO-PVS are shown in Fig. 2. Individuals with moderate and frequent/severe grade CSO-PVS had a higher diagnostic conversion risk than individuals with no/mild grade CSO-PVS (log-rank *p* < 0.001 for all) in the combined CN and MCI group. When stratified into separate CN and MCI groups, the risk difference of diagnostic conversion among CSO-PVS grades remained significant (log-rank *p* < 0.001 for all).

Further Cox regression analyses revealed that moderate and frequent/severe CSO-PVS were associated with a higher risk of diagnostic conversion (HR = 2.007, 95% CI = 1.382–2.914, *p* < 0.001; HR = 2.676, 95% CI = 1.830–3.911, *p* < 0.001, respectively) in the combined CN and MCI group. In the CN group, individuals with moderate and frequent/severe CSO-PVS had a higher progression rate to MCI/AD (HR = 2.023, 95% CI = 1.033–3.963, *p* = 0.040; HR = 3.504, 95% CI = 1.728–7.106, *p* < 0.001, respectively). In the MCI group, individuals with moderate and frequent/severe

Table 2 Group comparisons of MRI-visible PVS and other MRI findings across the Alzheimer's disease spectrum

	Data available	CN	Data available	MCI	Data available	AD	p value
CSO-PVS grade	486		667		276		<0.001 * ^{a,b,c}
No/mild (grades 0–1), n (%)		125 (25.7)		120 (18.0)		32 (11.6)	
Moderate (grade 2), n (%)		239 (49.2)		326 (48.9)		126 (45.7)	
Frequent/severe (grades 3–4), n (%)		122 (25.1)		221 (33.1)		118 (42.8)	
CSO-PVS number		15.9 (7.9)		17.5 (8.4)		19.0 (8.3)	<0.001 * ^{a,b,c}
BG-PVS grade	486		667		276		0.183
No/mild (grades 0–1), n (%)		399 (82.1)		531 (79.6)		221 (80.1)	
Moderate (grade 2), n (%)		78 (16.0)		126 (18.9)		45 (16.3)	
Frequent/severe (grades 3–4), n (%)		9 (1.9)		10 (1.5)		10 (3.6)	
BG-PVS number		7.2 (4.1)		7.4 (4.1)		7.7 (4.8)	0.326
HP-PVS grade	486		667		276		0.432
No/mild (0–1 PVS), n (%)		137 (28.2)		200 (30.0)		93 (33.7)	
Moderate (2–4 PVS), n (%)		217 (44.7)		290 (43.5)		122 (44.2)	
Frequent/severe (>4 PVS), n (%)		132 (27.2)		177 (26.5)		61 (22.1)	
HP-PVS number		3.2 (2.5)		3.0 (2.5)		2.8 (2.3)	0.182
WMH volume (cm ³)	486	1.25 (0.25, 3.91)	666	0.79 (0.20, 3.28)	275	1.14 (0.24, 3.93)	0.057
HP volume (cm ³)	483	7.33 (0.94)	653	6.57 (1.15)	262	5.60 (1.03)	<0.001 * ^{a,b,c}
Intracranial volume, cm ³	486	1415 (138)	665	1442 (145)	276	1420 (157)	0.005 * ^a

Values are reported as mean (standard deviation) for the quantitative variables except WMH volume which is reported as median (interquartile range). * $p < 0.05$. Group comparisons were done with the one-way ANOVA (quantitative variables) and chi-square test (categorical variables). WMH volume was log-transformed for one-way ANOVA analysis. ^a $p < 0.05$ between CN vs MCI. ^b $p < 0.05$ between CN vs AD. ^c $p < 0.05$ between MCI vs AD. CN control, MCI mild cognitive impairment, AD Alzheimer disease, CSO centrum semiovale, BG basal ganglia, HP hippocampus, PVS perivascular spaces, WMH white matter hyperintensities



CSO-PVS had a higher progression rate to AD (HR = 1.878, 95% CI = 1.197–2.947, $p = 0.006$; HR = 2.303, 95% CI = 1.462–3.628, $p < 0.001$, respectively).

Cross-sectional and longitudinal association between CSO-PVS and cognitive measures

Table 3 shows the cross-sectional and longitudinal

Table 3 Cross-sectional and longitudinal multiple linear regression of CSO-PVS with cognitive performance

	Total		CN		MCI		AD	
	β (95% CI)	<i>p</i> value	β (95% CI)	<i>p</i> value	β (95% CI)	<i>p</i> value	β (95% CI)	<i>p</i> value
Baseline								
ADAS-Cog 13	0.086 (0.044, 0.127)	<0.001*	0.009 (−0.033, 0.050)	0.677	0.060 (0.012, 0.107)	0.014*	0.042 (−0.063, 0.146)	0.432
MMSE	−0.161 (−0.205, −0.116)	<0.001*	−0.035 (−0.072, 0.002)	0.063	−0.151 (−0.201, −0.101)	<0.001*	−0.190 (−0.314, −0.065)	0.003*
ADNI-MEM	−0.093 (−0.133, −0.053)	<0.001*	−0.053 (−0.107, 0.001)	0.053	−0.060 (−0.112, −0.008)	0.023*	−0.020 (−0.092, 0.052)	0.585
ADNI-EF	−0.124 (−0.170, −0.077)	<0.001*	−0.128 (−0.193, −0.062)	<0.001*	−0.134 (−0.197, −0.071)	<0.001*	0.074 (−0.036, 0.185)	0.187
LME model								
ADAS-Cog 13	0.060 (0.026, 0.094)	0.001*	0.025 (0.002, 0.048)	0.032*	0.094 (0.046, 0.142)	<0.001*	0.015 (−0.164, 0.194)	0.870
MMSE	−0.069 (−0.108, −0.030)	0.001*	−0.054 (−0.081, −0.026)	<0.001*	−0.106 (−0.169, −0.043)	0.001*	0.287 (0.014, 0.559)	0.039*
ADNI-MEM	−0.058 (−0.090, −0.026)	<0.001*	−0.073 (−0.109, −0.037)	<0.001*	−0.043 (−0.092, 0.006)	0.085	0.018 (−0.126, 0.162)	0.805
ADNI-EF	−0.048 (−0.083, −0.012)	0.009*	−0.042 (−0.079, −0.006)	0.023*	−0.020 (−0.075, 0.035)	0.473	−0.088 (−0.308, 0.132)	0.432

Models were adjusted for age, sex, education, apo e4, hypertension, diabetes, hyperlipidemia, coronary heart disease, atrial fibrillation, smoking, WMH volume, hippocampus volume, and intracranial volume. Continuous independent variables and covariates in the models were z-scored prior to analysis for standardization. In the LME model, CSO-PVS*time was the effect of interest, as it reflected whether CSO-PVS moderated the relationship between time and cognitive decline. * $p < 0.05$. CSO centrum semiovale, PVS perivascular spaces, CN control, MCI mild cognitive impairment, AD Alzheimer disease, ADAS-Cog 13 13-item Alzheimer's Disease Assessment Scale-cognitive subscale, MMSE Mini-Mental State Examination, ADNI-MEM ADNI memory composite score, ADNI-EF ADNI executive function score, ADNI Alzheimer's Disease Neuroimaging Initiative, LME linear mixed-effects model

association between CSO-PVS and cognitive measures. In the cross-sectional analysis, a higher CSO-PVS number was positively associated with ADAS-Cog 13 ($\beta = 0.086$, $p < 0.001$; $\beta = 0.060$, $p = 0.014$) and negatively associated with MMSE ($\beta = -0.161$, $p < 0.001$; $\beta = -0.151$, $p < 0.001$), ADNI-MEM ($\beta = -0.093$, $p < 0.001$; $\beta = -0.060$, $p = 0.023$), and ADNI-EF ($\beta = -0.124$, $p < 0.001$; $\beta = -0.134$, $p < 0.001$) in all subjects and in the MCI group. The association remained significant with ADNI-EF in the CN group ($\beta = -0.128$, $p < 0.001$) and MMSE in the AD group ($\beta = -0.190$, $p < 0.003$). The detailed beta coefficients for all variables in the regression models can be found in Supplementary Tables 2, 3, 4 and 5.

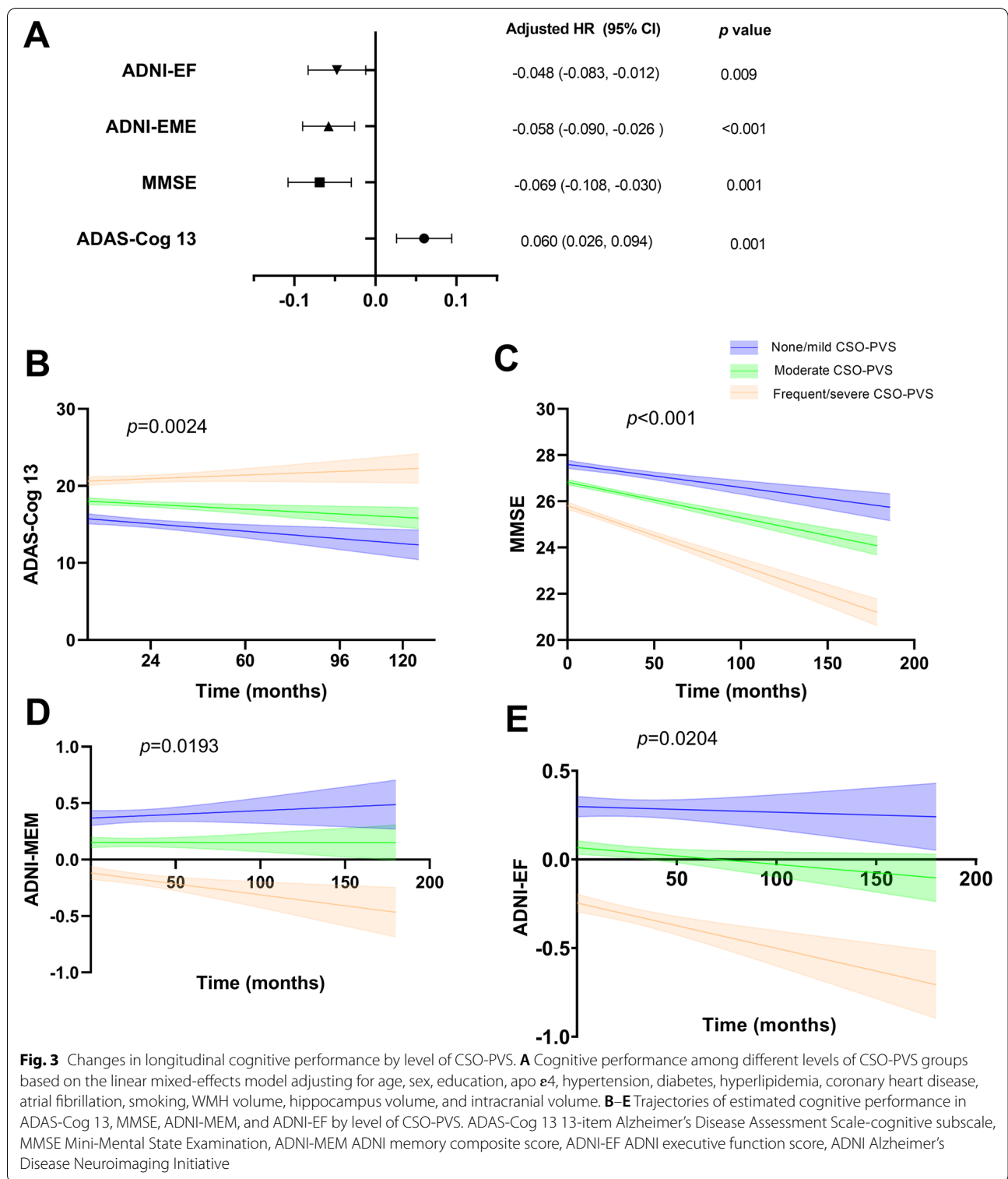
LME models showed that a higher CSO-PVS number was associated with cognitive decline in the ADAS-Cog 13 ($\beta = 0.060$, $p = 0.001$; $\beta = 0.025$, $p = 0.032$), MMSE ($\beta = -0.069$, $p = 0.001$; $\beta = -0.054$, $p < 0.001$), ADNI-MEM ($\beta = -0.058$, $p < 0.001$; $\beta = -0.073$, $p < 0.001$), and ADNI-EF ($\beta = -0.048$, $p = 0.009$; $\beta = -0.042$, $p = 0.023$) in all subjects and in the CN group. The association remained significant with ADAS-Cog 13 ($\beta = 0.094$, $p < 0.001$) and MMSE ($\beta = -0.106$, $p = 0.001$) scores in the MCI group and MMSE scores in the AD group ($\beta = 0.287$, $p = 0.039$). The detailed beta coefficients for all the variables in the regression models can be found in Supplementary Tables 6, 7, 8 and 9. As shown in Fig. 3, individuals with moderate and frequent/severe CSO-PVS

had a more rapid decline in all cognitive measures than subjects with no/mild CSO-PVS.

Discussion

In this study, we investigated the characteristics and associations of MRI-visible PVS with clinical progression and longitudinal cognitive decline across the AD spectrum. Our study found that MCI and AD subjects had more CSO-PVS than CN subjects. Individuals with moderate and frequent/severe grade CSO-PVS had a more than 2-fold higher clinical progression risk than individuals with no/mild grade CSO-PVS. A higher CSO-PVS number was associated with baseline cognitive performance and longitudinal cognitive decline in all cognitive tests.

With the wide use of MRI, MRI-visible PVS are frequently detected in clinical practice. Emerging literature suggests that arterial stiffening and abnormal protein aggregation in vessel walls are two potential mechanisms that drive PVS formation [28]. Arterial stiffening, influenced by age, hypertension, and other cardiovascular diseases, was shown to have an association with BG-PVS [29–31]. Notably, CSO-PVS and HP-PVS may also be affected by cardiovascular risk factors and cerebral small vessel disease [32, 33]. Regarding abnormal protein aggregation, CSO-PVS was proven to be most commonly affected in cerebral amyloid angiopathy (CAA) with A β deposition [34].



In our study, compared with CN subjects, MCI and AD subjects had more CSO-PVS both in number and grade. This was similar to previous studies [18–20]. Notably, a recent study using a quantitative method also revealed

that MCI subjects had more CSO-PVS than normal controls [35]. A high degree of CSO-PVS has been suggested to be associated with CAA, which is characterized by neurovascular accumulation of A β and deficiencies in the

clearance of A β along the arterial perivascular space [36, 37]. A postmortem AD sample study showed increased PVS and global AQP4 expression with a qualitative reduction in perivascular localization of AQP4 in frontal cortical tissue compared with control subjects, and increasing PVS burden was associated with the presence of tau and A β pathology [38]. As AQP4 has a clear role in brain glymphatic pathway function [39], PVS may reflect failed glymphatic function leading to clearance deficiency in parenchymal A β and other brain waste in AD.

However, there was no significant difference in BG-PVS across the AD spectrum. BG-PVS was more related to hypertensive arteriopathy [40, 41] and vascular dementia [20, 42]. As there was no significant difference in cardiovascular disease history across the AD spectrum in our study, the effect of cardiovascular disease on BG-EPVS could be neglectable. Our study suggested no association between BG-PVS and the AD spectrum. Furthermore, we found no significant difference in HP-PVS among the AD spectrum. Previous studies suggested that age and hypertension were the two main factors associated with HP-PVS [32, 43, 44], and HP-PVS was not associated with the occurrence of dementia [32]. The development of MRI-visible HP-PVS may have little association with AD. However, a small sample size (39 AD patients) study found increased HP-PVS but no significant difference in CSO-PVS in AD [21]. The contradictory results may be caused by different study designs and enrolled populations. The enrolled population in their study tended to have more cardiovascular disease, which would have a nonnegligible effect on the occurrence of MRI-visible PVS.

Regarding the relationship between MRI-visible PVS and cognitive impairment, there were mixed findings. Two meta-analyses found no association of MRI-visible PVS with cognitive impairment cross-sectionally [45, 46]. However, a longitudinal study revealed that severe MRI-visible PVS, especially CSO-PVS, was associated with an increased risk of cognitive decline and dementia in community-dwelling older adults [47], and a recent study revealed that CSO-PVS was associated with the progression of cognitive decline in an amyloid-independent manner in the AD continuum [48]. In our study, CSO-PVS was also associated with baseline cognitive performance and longitudinal cognitive decline in all subjects after adjusting for cardiovascular disease and other risk factors, indicating that there was an independent association of CSO-PVS with cognitive impairment. As mentioned above, we speculated that CSO-PVS may represent impaired glymphatic function causing clearance deficiency of amyloid and other toxins, leading to cognitive impairment. However, some cognitive tests were not associated with CSO-PVS in the separate CN,

MCI, and AD group analyses. We speculate that the weak associations may be caused by less statistical power in the separate group analysis, while the disease severity would mediate the relationship between CSO-PVS and cognition in the combined analysis. Future studies using more sensitive methods, such as quantitative CSO-PVS volume analyses in separate groups, are warranted to replicate our results.

Interestingly, individuals with moderate and frequent/severe grade CSO-PVS had a more than 2-fold higher diagnostic conversion risk than individuals with no/mild grade CSO-PVS in the CN and MCI groups. In the CN group, individuals with frequent/severe CSO-PVS even had a more than 3-fold higher progression rate to MCI/AD than individuals with no/mild grade CSO-PVS. To our knowledge, this was the first study to investigate the value of MRI-visible PVS in the diagnostic conversion risk across the AD spectrum. Our study suggested the role of CSO-PVS in the development of AD and provided a potential novel imaging biomarker for disease severity assessment.

Our study should be interpreted in light of the following limitations. First, the ADNI project had strict inclusion and exclusion criteria, and the enrolled subjects were not representative of the wider general population [49]. This may be considered an advantage, as the sample represented a relatively pure sample with little confounding. However, the results may not necessarily ensure generalizability. Second, A β and tau biomarkers were not investigated in the relationship between MRI-visible PVS and cognitive impairment. A β and tau may play an important role in the relationship. However, there were too many missing data about CSF or PET biomarkers of A β and tau. Future research on the role of A β and tau in the relationship between MRI-visible PVS and cognitive impairment is warranted. Third, PVS in the hippocampus are very difficult to distinguish from hippocampal sulcus remnant cysts [50]. The results of MRI-visible PVS in the hippocampus should be interpreted with caution. Fourth, no quantitative analysis was performed to assess PVS, and we only used validated visual rating scales, which were rater-dependent and had ceiling or floor effects. However, the assessment method was simple, and the interrater and intra-rater reliability for the rating of MRI-visible PVS was excellent. The visual rating method could be applied easily in clinical practice.

In conclusion, our study demonstrated that CSO-PVS were more common in MCI and AD. CSO-PVS were associated with cognitive decline across the AD spectrum. Our study suggested that MRI-visible PVS could be a novel imaging assessment biomarker and a new potential therapeutic target for cognitive decline in the AD spectrum.

Supplementary Information

The online version contains supplementary material available at <https://doi.org/10.1186/s13195-022-01136-y>.

Additional file 1: Supplementary table 1. Demographics and Clinical Characteristics across the Alzheimer's disease spectrum between included and excluded subjects.

Additional file 2: Supplementary table 2. Cross-sectional multivariable linear regression of CSO-PVS with ADAS-Cog 13 across the Alzheimer's disease spectrum.

Additional file 3: Supplementary table 3. Cross-sectional multivariable linear regression of CSO-PVS with MMSE across the Alzheimer's disease spectrum.

Additional file 4: Supplementary table 4. Cross-sectional multivariable linear regression of CSO-PVS with ADNI-MEM across the Alzheimer's disease spectrum.

Additional file 5: Supplementary table 5. Cross-sectional multivariable linear regression of CSO-PVS with ADNI-EF across the Alzheimer's disease spectrum.

Additional file 6: Supplementary table 6. Longitudinal linear mixed-effects regression of CSO-PVS with ADAS-13 across the Alzheimer's disease spectrum.

Additional file 7: Supplementary table 7. Longitudinal linear mixed-effects regression of CSO-PVS with MMSE across the Alzheimer's disease spectrum.

Additional file 8: Supplementary table 8. Longitudinal linear mixed-effects regression of CSO-PVS with ADNI-MEM across the Alzheimer's disease spectrum.

Additional file 9: Supplementary table 9. Longitudinal linear mixed-effects regression of CSO-PVS with ADNI-EF across the Alzheimer's disease spectrum.

Acknowledgements

The authors thank Meng-Meng Yu, MD, of the Department of Radiology at Zhongshan Hospital, Fudan University for her help in manuscript revision and statistical analyses in the study. Data collection and sharing for this project was funded by the Alzheimer's Disease Neuroimaging Initiative (ADNI) (National Institutes of Health Grant U01 AG024904) and DOD ADNI (Department of Defense award number W81XWH-12-2-0012). ADNI is funded by the National Institute on Aging, the National Institute of Biomedical Imaging and Bioengineering, and through generous contributions from the following: AbbVie, Alzheimer's Association; Alzheimer's Drug Discovery Foundation; Araclon Biotech; Bio Clinica, Inc.; Biogen; Bristol-Myers Squibb Company; CereSpir, Inc.; Cogstate; Eisai Inc.; Elan Pharmaceuticals, Inc.; Eli Lilly and Company; EuroImmun; F. Hoffmann-La Roche Ltd and its affiliated company Genentech, Inc.; Fujirebio; GE Healthcare; IXICO Ltd.; Janssen Alzheimer Immunotherapy Research & Development, LLC.; Johnson & Johnson Pharmaceutical Research & Development LLC.; Lumosity; Lundbeck; Merck & Co., Inc.; Meso Scale Diagnostics, LLC.; NeuroRx Research; Neurotrack Technologies; Novartis Pharmaceuticals Corporation; Pfizer Inc.; Piramal Imaging; Servier; Takeda Pharmaceutical Company; and Transition Therapeutics. The Canadian Institutes of Health Research is providing funds to support ADNI clinical sites in Canada. Private sector contributions are facilitated by the Foundation for the National Institutes of Health (www.fnih.org). The grantee organization is the Northern California Institute for Research and Education, and the study is coordinated by the Alzheimer's Therapeutic Research Institute at the University of Southern California. ADNI data are disseminated by the Laboratory for Neuro Imaging at the University of Southern California.

Authors' contributions

ML W and YH L: study concept and design; ML W, QQ Z, and XE W: analysis and interpretation of data and drafting of the manuscript; ML W, QQ Z, PY L, and X W: statistical analysis and critical revision of the manuscript. YH L: administrative, technical, and material support and study supervision. All authors give final approval of the version published.

Funding

This study was supported by the National Key Research and Development Program of China (2019YFC0117703), National Natural Science Foundation of China (81901727), New developing and Frontier Technologies of Shanghai Shen Kang Hospital Development Center (SHDC12018117), Shanghai Municipal Education Commission-Gaofeng Clinical Medicine Grant Support (2016427), Excellent discipline leader of Shanghai Municipal Planning Commission (2017BR041), and Shanghai key discipline of medical imaging (2017ZZ02005).

Availability of data and materials

All imaging, demographics, and neuropsychological data used in this article are publicly available and were downloaded from the ADNI website (adni.loni.usc.edu). Upon request, we will provide a list of ADNI participant identifications for replication purposes.

Declarations

Ethics approval and consent to participate

The ADNI project was approved by the institutional review boards of all participating ADNI sites. Written informed consent was obtained from all the participants or their authorized representatives in accordance with the Declaration of Helsinki.

Consent for publication

Not applicable.

Competing interests

The authors declare no competing interests.

Author details

¹Department of Radiology, Shanghai Sixth People's Hospital Affiliated to Shanghai Jiao Tong University School of Medicine, No. 600, Yi Shan Road, Shanghai 200233, China. ²Division of Cardiology, Pauley Heart Center, Virginia Commonwealth University, Richmond, VA, USA. ³Institute for Global Health Sciences, University of California San Francisco, San Francisco, CA, USA.

Received: 15 May 2022 Accepted: 5 December 2022

Published online: 13 December 2022

References

- Scheltens P, De Strooper B, Kivipelto M, Holstege H, Chételat G, Teunissen CE, et al. Alzheimer's disease. *Lancet*. 2021;397(10284):1577–90.
- Zhang F, Zhong RJ, Cheng C, Li S, Le WD. New therapeutics beyond amyloid- β and tau for the treatment of Alzheimer's disease. *Acta Pharmacol Sin*. 2021;42(9):1382–9.
- Plog BA, Nedergaard M. The glymphatic system in central nervous system health and disease: past, present, and future. *Annu Rev Pathol*. 2018;13:379–94.
- Wardlaw JM, Benveniste H, Nedergaard M, Zlokovic BV, Mestre H, Lee H, et al. Perivascular spaces in the brain: anatomy, physiology and pathology. *Nat Rev Neurol*. 2020;16(3):137–53.
- Kwee RM, Kwee TC. Virchow-Robin spaces at MR imaging. *Radiographics*. 2007;27(4):1071–86.
- Doubal FN, MacLulich AM, Ferguson KJ, Dennis MS, Wardlaw JM. Enlarged perivascular spaces on MRI are a feature of cerebral small vessel disease. *Stroke*. 2010;41(3):450–4.
- Iliff JJ, Wang M, Liao Y, Plogg BA, Peng W, Gundersen GA, et al. A paravascular pathway facilitates CSF flow through the brain parenchyma and the clearance of interstitial solutes, including amyloid β . *Sci Transl Med*. 2012;4(147):147ra11.
- Rasmussen MK, Mestre H, Nedergaard M. The glymphatic pathway in neurological disorders. *Lancet Neurol*. 2018;17(11):1016–24.
- Venkat P, Chopp M, Zacharek A, Cui C, Zhang L, Li Q, et al. White matter damage and glymphatic dysfunction in a model of vascular dementia in rats with no prior vascular pathologies. *Neurobiol Aging*. 2017;50:96–106.

10. Shen T, Yue Y, Zhao S, Xie J, Chen Y, Tian J, et al. The role of brain perivascular space burden in early-stage Parkinson's disease. *NPJ Parkinsons Dis*. 2021;7(1):12.
11. Li Y, Zhu Z, Chen J, Zhang M, Yang Y, Huang P. Dilated perivascular space in the midbrain may reflect dopamine neuronal degeneration in Parkinson's disease. *Front Aging Neurosci*. 2020;12:161.
12. Donahue EK, Murdos A, Jakowec MW, Sheikh-Bahaei N, Toga AW, Petzinger GM, et al. Global and regional changes in perivascular space in idiopathic and familial Parkinson's disease. *Mov Disord*. 2021;36(5):1126–36.
13. Chan ST, Mercaldo ND, Ravina B, Hersch SM, Rosas HD. Association of dilated perivascular spaces and disease severity in patients with Huntington disease. *Neurology*. 2021;96(6):e890–e4.
14. Wang ML, Sun Z, Li WB, Zou QQ, Li PY, Wu X, et al. Enlarged perivascular spaces and white matter hyperintensities in patients with frontotemporal lobar degeneration syndromes. *Front Aging Neurosci*. 2022;14:923193.
15. Lyndon D, Davagnanam I, Wilson D, Jichi F, Merwick A, Bolsover F, et al. MRI-visible perivascular spaces as an imaging biomarker in Fabry disease. *J Neurol*. 2021;268(3):872–8.
16. Wang M-L, Yu M-M, Wei X-E, Li W-B, Li Y-H. Association of enlarged perivascular spaces with A β and tau deposition in cognitively normal older population. *Neurobiol Aging*. 2021;100:32–8.
17. Wang ML, Yang DX, Sun Z, Li WB, Zou QQ, Li PY, et al. MRI-visible perivascular spaces associated with cognitive impairment in military veterans with traumatic brain injury mediated by CSF P-tau. *Front Psychiatry*. 2022;13:921203.
18. Chen W, Song X, Zhang Y. Assessment of the Virchow-Robin spaces in Alzheimer disease, mild cognitive impairment, and normal aging, using high-field MR imaging. *AJNR Am J Neuroradiol*. 2011;32(8):1490–5.
19. Ramirez J, Berezuk C, McNeely AA, Scott CJ, Gao F, Black SE. Visible Virchow-Robin spaces on magnetic resonance imaging of Alzheimer's disease patients and normal elderly from the Sunnybrook Dementia Study. *J Alzheimers Dis*. 2015;43(2):415–24.
20. Banerjee G, Kim HJ, Fox Z, Jäger HR, Wilson D, Charidimou A, et al. MRI-visible perivascular space location is associated with Alzheimer's disease independently of amyloid burden. *Brain*. 2017;140(4):1107–16.
21. Gertje EC, van Westen D, Panizo C, Mattsson-Carligen N, Hansson O. Association of enlarged perivascular spaces and measures of small vessel and Alzheimer disease. *Neurology*. 2021;96(2):e193–202.
22. Petersen RC, Aisen PS, Beckett LA, Donohue MC, Gamst AC, Harvey DJ, et al. Alzheimer's Disease Neuroimaging Initiative (ADNI): clinical characterization. *Neurology*. 2010;74(3):201–9.
23. Crane PK, Carle A, Gibbons LE, Insel P, Mackin RS, Gross A, et al. Development and assessment of a composite score for memory in the Alzheimer's Disease Neuroimaging Initiative (ADNI). *Brain Imaging Behav*. 2012;6(4):502–16.
24. Gibbons LE, Carle AC, Mackin RS, Harvey D, Mukherjee S, Insel P, et al. A composite score for executive functioning, validated in Alzheimer's Disease Neuroimaging Initiative (ADNI) participants with baseline mild cognitive impairment. *Brain Imaging Behav*. 2012;6(4):517–27.
25. Wardlaw JM, Smith EE, Biessels GJ, Cordonnier C, Fazekas F, Frayne R, et al. Neuroimaging standards for research into small vessel disease and its contribution to ageing and neurodegeneration. *Lancet Neurol*. 2013;12(8):822–38.
26. MacLullich AM, Wardlaw JM, Ferguson KJ, Starr JM, Seckl JR, Deary IJ. Enlarged perivascular spaces are associated with cognitive function in healthy elderly men. *J Neurol Neurosurg Psychiatry*. 2004;75(11):1519–23.
27. Potter GM, Chappell FM, Morris Z, Wardlaw JM. Cerebral perivascular spaces visible on magnetic resonance imaging: development of a qualitative rating scale and its observer reliability. *Cerebrovasc Dis (Basel, Switzerland)*. 2015;39(3–4):224–31.
28. Bown CW, Carare RO, Schrag MS, Jefferson AL. Physiology and clinical relevance of enlarged perivascular spaces in the aging brain. *Neurology*. 2022;98(3):107–17.
29. Riba-Llena I, Jiménez-Balado J, Castañé X, Girona A, López-Rueda A, Mundet X, et al. Arterial stiffness is associated with basal ganglia enlarged perivascular spaces and cerebral small vessel disease load. *Stroke*. 2018;49(5):1279–81.
30. Potter GM, Doubal FN, Jackson CA, Chappell FM, Sudlow CL, Dennis MS, et al. Enlarged perivascular spaces and cerebral small vessel disease. *Int J Stroke*. 2015;10(3):376–81.
31. Choi EY, Park YW, Lee M, Kim M, Lee CS, Ahn SS, et al. Magnetic resonance imaging-visible perivascular spaces in the basal ganglia are associated with the diabetic retinopathy stage and cognitive decline in patients with type 2 diabetes. *Front Aging Neurosci*. 2021;13:666495.
32. Yao M, Zhu YC, Soumaré A, Dufouil C, Mazoyer B, Tzourio C, et al. Hippocampal perivascular spaces are related to aging and blood pressure but not to cognition. *Neurobiol Aging*. 2014;35(9):2118–25.
33. Wang S, Huang P, Zhang R, Hong H, Jiaerken Y, Lian C, et al. Quantity and morphology of perivascular spaces: associations with vascular risk factors and cerebral small vessel disease. *J Magn Reson Imaging*. 2021;54(4):1326–36.
34. Perosa V, Oltmer J, Munting LP, Freeze WM, Auger CA, Scherlek AA, et al. Perivascular space dilation is associated with vascular amyloid- β accumulation in the overlying cortex. *Acta Neuropathol*. 2022;143(3):331–48.
35. Sepehrband F, Barisano G, Sheikh-Bahaei N, Choupan J, Cabeen RP, Lynch KM, et al. Volumetric distribution of perivascular space in relation to mild cognitive impairment. *Neurobiol Aging*. 2021;99:28–43.
36. van Veluw SJ, Biessels GJ, Bouvy WH, Spliet WG, Zwanenburg JJ, Luijten PR, et al. Cerebral amyloid angiopathy severity is linked to dilation of juxtacortical perivascular spaces. *J Cereb Blood Flow Metab*. 2016;36(3):576–80.
37. Charidimou A, Boulouis G, Pasi M, Auriel E, van Etten ES, Haley K, et al. MRI-visible perivascular spaces in cerebral amyloid angiopathy and hypertensive arteriopathy. *Neurology*. 2017;88(12):1157–64.
38. Boespflug EL, Simon MJ, Leonard E, Grafe M, Woltjer R, Silbert LC, et al. Targeted assessment of enlargement of the perivascular space in Alzheimer's disease and vascular dementia subtypes implicates astroglial involvement specific to Alzheimer's disease. *J Alzheimers Dis*. 2018;66(4):1587–97.
39. Mestre H, Hablitz LM, Xavier AL, Feng W, Zou W, Pu T, et al. Aquaporin-4-dependent glymphatic solute transport in the rodent brain. *eLife*. 2018;7:e40070.
40. Yakushiji Y, Charidimou A, Hara M, Noguchi T, Nishihara M, Eriguchi M, et al. Topography and associations of perivascular spaces in healthy adults: the Kashima scan study. *Neurology*. 2014;83(23):2116–23.
41. Charidimou A, Meegahage R, Fox Z, Peeters A, Vandermeeren Y, Laloux P, et al. Enlarged perivascular spaces as a marker of underlying arteriopathy in intracerebral haemorrhage: a multicentre MRI cohort study. *J Neurol Neurosurg Psychiatry*. 2013;84(6):624–9.
42. Shams S, Martola J, Charidimou A, Larvie M, Granberg T, Shams M, et al. Topography and determinants of magnetic resonance imaging (MRI)-visible perivascular spaces in a large memory clinic cohort. *J Am Heart Assoc*. 2017;6(9):e006279.
43. Zhang C, Chen Q, Wang Y, Zhao X, Wang C, Liu L, et al. Risk factors of dilated Virchow-Robin spaces are different in various brain regions. *PLoS One*. 2014;9(8):e105505.
44. Jiménez-Balado J, Riba-Llena I, Garde E, Valor M, Gutiérrez B, Pujadas F, et al. Prevalence of hippocampal enlarged perivascular spaces in a sample of patients with hypertension and their relation with vascular risk factors and cognitive function. *J Neurol Neurosurg Psychiatry*. 2018;89(6):651–6.
45. Hilal S, Tan CS, Adams HHH, Habes M, Mok V, Venketasubramanian N, et al. Enlarged perivascular spaces and cognition: a meta-analysis of 5 population-based studies. *Neurology*. 2018;91(9):e832–e42.
46. Francis F, Ballerini L, Wardlaw JM. Perivascular spaces and their associations with risk factors, clinical disorders and neuroimaging features: a systematic review and meta-analysis. *Int J Stroke*. 2019;14(4):359–71.
47. Paradise M, Crawford JD, Lam BCP, Wen W, Kochan NA, Makkar S, et al. Association of dilated perivascular spaces with cognitive decline and incident dementia. *Neurology*. 2021;96(11):e1501–e11.
48. Young JJ, Jensen RK, Hartvigsen J, Roos EM, Ammendolia C, Juhl CB. Prevalence of multimorbid degenerative lumbar spinal stenosis with knee or hip osteoarthritis: a systematic review and meta-analysis. *BMC Musculoskelet Disord*. 2022;23(1):177.
49. Veitch DP, Weiner MW, Aisen PS, Beckett LA, DeCarli C, Green RC, et al. Using the Alzheimer's Disease Neuroimaging Initiative to improve early detection, diagnosis, and treatment of Alzheimer's disease. *Alzheimers Dementia*. 2022;18(4):824–57.
50. Barisano G, Lynch KM, Sibilia F, Lan H, Shih NC, Sepehrband F, et al. Imaging perivascular space structure and function using brain MRI. *Neuroimage*. 2022;257:119329.

Publisher's Note

Springer Nature remains neutral with regard to jurisdictional claims in published maps and institutional affiliations.